Molecular Cell
Article

Mechanism of Translesion Transcription by RNA Polymerase II and Its Role in Cellular Resistance to DNA Damage

Celine Walmacq,[1] Alan C.M. Cheung,[2] Maria L. Kireeva,[1] Lucyna Lubkowska,[1] Chengcheng Ye,[1] Deanna Gotte,[1] Jeffrey N. Strathern,[1] Thomas Carell,[3] Patrick Cramer,[2] and Mikhail Kashlev[1,*]
[1]NCI Center for Cancer Research, Frederick, MD 21702, USA
[2]Gene Center and Department of Biochemistry, Center for Integrated Protein Science CIPSM, Ludwig-Maximilians-Universität München, Feodor-Lynen-Strasse 25, 81377 Munich, Germany
[3]Department of Chemistry, Center for Integrated Protein Science CIPSM, Ludwig-Maximilians-Universität München, Butenandt-Strasse 5-13, 81377 Munich, Germany
*Correspondence: mkashlev@mail.ncifcrf.gov
DOI 10.1016/j.molcel.2012.02.006

SUMMARY

UV-induced cyclobutane pyrimidine dimers (CPDs) in the template DNA strand stall transcription elongation by RNA polymerase II (Pol II). If the nucleotide excision repair machinery does not promptly remove the CPDs, stalled Pol II creates a roadblock for DNA replication and subsequent rounds of transcription. Here we present evidence that Pol II has an intrinsic capacity for translesion synthesis (TLS) that enables bypass of the CPD with or without repair. Translesion synthesis depends on the trigger loop and bridge helix, the two flexible regions of the Pol II subunit Rpb1 that participate in substrate binding, catalysis, and translocation. Substitutions in Rpb1 that promote lesion bypass in vitro increase UV resistance in vivo, and substitutions that inhibit lesion bypass decrease cell survival after UV irradiation. Thus, translesion transcription becomes essential for cell survival upon accumulation of the unrepaired CPD lesions in genomic DNA.

INTRODUCTION

DNA damage caused by UV irradiation or chemical modifications affects all DNA transactions, including replication and transcription. Single- and double-strand breaks, along with the various DNA lesions, can interfere with the progression of DNA and RNA polymerases and compromise fidelity of genetic information transfer (Friedberg, 1996). Therefore, cells have evolved an orchestrated interplay of various DNA repair mechanisms to prevent the life-threatening disruption of replication and transcription by DNA damage. Nonbulky and non-helix-distorting DNA lesions are preferentially removed by base excision repair while damage that causes large DNA distortion, such as UV-induced cyclobutane pyrimidine dimers (CPDs) are subject to the nucleotide-excision repair (NER) pathway (Hoeijmakers, 2001). Despite ongoing DNA repair, some lesions escape detection and pose a potentially lethal roadblock for both replication and transcription machineries. Therefore, cell resistance to UV irradiation depends on the efficiency of all the DNA repair pathways, and on the ability of the replication and transcription machineries to bypass sites of unrepaired DNA damage.

DNA damage, such as abasic sites or *cis-syn* CPDs, typically causes replication fork arrest, which does not necessarily promote lesion repair. Interestingly, replicative DNA polymerases preferentially insert an adenine nucleotide opposite noninstructional abasic sites according to the A-rule (Strauss, 1991; Taylor, 2002). Structures of DNA polymerases in complex with DNA containing *cis-syn* CPD revealed the highly constrained shape of the active site, which only accommodates a single template base and prevents damaged template bases from entering the active site (Li et al., 2004). Consistently, replicative polymerases catalyze nontemplated adenine insertion opposite the first thymine of the CPD (3′T) when the lesion is excluded from the active center, but catalyze template-directed adenine insertion opposite the second thymine (5′T) when the lesion occupies the active site (Li et al., 2004).

Replication can be restarted and the deleterious effect of DNA lesions alleviated by translesion DNA synthesis. During translesion synthesis (TLS), the high-fidelity replicative DNA polymerases are transiently replaced by translesion DNA polymerases (reviewed in Waters et al., 2009).The relaxed active site of translesion polymerases can accommodate various damaged template bases, thus enabling their bypass. Compared to the replicative DNA polymerases, translesion polymerases lack a 3′ to 5′ proofreading exonuclease activity and have reduced fidelity when replicating undamaged DNA, with error rates ranging from 10^{-1} to 10^{-5}. Consequently, the undamaged DNA replication by translesion polymerases is potentially mutagenic. However, certain translesion polymerases replicate across particular DNA lesions in an error-free manner and with a high efficiency of nucleotide insertion opposite the lesion. The error-free activity of DNA Pol η in bypassing UV-induced lesions is critical for the avoidance of sunlight-induced skin cancers in humans (Waters et al., 2009).

An encounter of RNA polymerase with DNA lesions triggers transcription-coupled nucleotide excision repair (TC-NER), which efficiently removes bulky lesions from the transcribed

strand (Bohr et al., 1985; Mellon et al., 1987). Pol II stalled at a lesion recruits the repair machinery (Hanawalt and Spivak, 2008). Recruitment of the repair factors is necessary but not sufficient for lesion removal, because the DNA lesion is buried within the stalled RNA polymerase and is not accessible to the proteins that conduct repair (Brueckner et al., 2007). The damaged DNA strand may be excised in the presence of Pol II (Brueckner et al., 2007), or Pol II may be removed from the lesion by proteolytic degradation (Woudstra et al., 2002) or by a backward movement of the elongation complex. Lesion bypass is considered an alternative possibility during TC-NER (Hanawalt and Spivak, 2008). Indeed, RNA polymerase can bypass various types of DNA damage, such as abasic sites or single-strand breaks, however with a likelihood of transcriptional mutagenesis (Saxowsky and Doetsch, 2006).

In principle, there are three different outcomes of Pol II negotiation with a lesion: (i) stalling due to a block of translocation into the active site, as seen for the bulky *cis-platin* lesion (Damsma et al., 2007) (ii) stalling due to nucleotide misincorporation opposite the lesion, as observed for the CPD (Brueckner et al., 2007), or (iii) bypass, as observed for small lesions like 8-oxoG (Damsma and Cramer, 2009). Although bulky DNA photoproducts such as CPDs efficiently stall transcription in vitro (Brueckner et al., 2007; Donahue et al., 1994), several lines of evidence suggest that CPDs do not constitute absolute blocks to transcription in vivo (Brooks et al., 2000; Ljungman and Zhang, 1996; Marietta and Brooks, 2007). However, the physiological significance and mechanism of any translesion transcription for bulky lesions remains poorly understood.

In this work, we address the mechanism of DNA lesion bypass by Pol II and its role in cell survival after UV irradiation. For analysis of translesion transcription, we used mutant variants of Pol II with antagonistic elongation defects and with altered transcription fidelity. Our findings reveal striking similarities between the mechanisms of TLS by Pol II and that for replicative and translesion DNA polymerases. Thus, lesion bypass by Pol II represents a housekeeping mechanism for DNA damage tolerance. We also provide the first evidence that TLS may represent a mechanism for exposure of the lesions to TC-NER proteins as an alternative to ubiquitin-mediated degradation of Pol II.

RESULTS

CPD Bypass Correlates with Increased Cellular UV Resistance

Mutations in the catalytic Rpb1 subunit of Pol II that alter the active center flexibility and cause defects in the rate of bond formation and transcription fidelity provide a unique tool to investigate possible TLS by Pol II. In this work, we used mutant polymerases Rpb1-E1103G and Rpb1-G730D with antagonistic elongation defect and altered transcription fidelity. In vitro transcription assays showed that Rpb1-E1103G mutation increases the bulk rate of elongation by Pol II by 3-fold while Rpb1-G730D mutation confers a severe 10-fold decrease of the transcription rate (Supplemental Information and Figure S1A). The E1103 residue in Rpb1 controls transcription fidelity by stabilizing the open or destabilizing the closed conformation of the trigger loop (TL) (Kireeva et al., 2008), a flexible element of Pol II catalytic center that encloses the incoming NTP (Figure 1A) (Kaplan et al., 2008; Wang et al., 2006). The E1103G mutation decreases transcription fidelity in vitro and in vivo, possibly by promoting the TL closure over mispaired bases (Kireeva et al., 2008). Similarly to E1103G substitution, Rpb1-G730D mutation substantially decreased fidelity in vitro (Supplemental Information and Figure S1B). Note that this mutation was reported to increase fidelity in vivo (Koyama et al., 2010). We discussed possible explanations for this discrepancy in the Supplemental Information. The Rpb1-G730 residue is positioned in the long α21 helix, which forms a part of the secondary pore in the enzyme and contacts the TL (Figure 1A) (Cramer et al., 2001). Rpb1-G730D may affect the proper alignment of the β/γ phosphate moiety of the incoming NTP with the 3′OH group of the RNA required for catalysis, thus resulting in decreased fidelity (Supplemental Information and Figure S1C). Thus, both mutations alter the catalytic activity of Pol II in the opposite ways and render Pol II error-prone, most likely through different mechanisms (Supplemental Information and Figure S1).

First, we analyzed the effects of the mutations in the Rpb1 subunit on UV sensitivity of *S. cerevisiae.* We constructed yeast strains in a *rad16* background that carried wild-type *RPB1*, *rpb1-E1103G*, and *rpb1-G730D* mutations. *RAD16* encodes an essential component of an efficient global genomic nucleotide excision repair pathway (GG-NER). *RAD16* deletion leads to a significant increase of the cell sensitivity to UV (Supplemental Information and Figure S1D), rendering the cells more dependent on the less efficient TC-NER pathway, which requires the functional *RAD26 gene* (van Gool et al., 1994). In the *rad16* mutant background, changes in the rate of transcription and fidelity have a significant impact on cell sensitivity to UV irradiation. Specifically, the *rpb1-E1103G* mutation confers UV resistance whereas *rpb1-G730D* mutation exacerbates the UV sensitivity (Figure 1B). These results suggest a direct correlation between Pol II catalytic activity and UV sensitivity when the GG-NER is abolished. This correlation could be explained in at least two ways: the altered Pol II behavior and fidelity at DNA lesions might (i) directly affect the DNA repair by TC-NER and GG-NER and/or (ii) prevent/amplify the lethal consequences of the unrepaired lesion accumulation.

CPD lesions are the most common type of chemical DNA damage induced by UV light. To investigate how the Pol II mutations could affect UV sensitivity, we tested the ability of the purified wild-type and mutant polymerases to transcribe a single CPD located in the template DNA strand (Figure 1C). We monitored RNA extension using a promoter-independent assay with CPD-stalled ternary elongation complexes carrying a 12 nt transcript (TEC12). The TECs were reconstituted with *S. cerevisiae* Pol II and nucleic acid scaffolds as described previously (Walmacq et al., 2009), and incubated with physiological concentration of NTPs. The majority of the TECs stalled after incorporation of a nucleotide opposite the first thymidine (3′T) of the lesion (Figure 1C), which was in general agreement with previous reports (Donahue et al., 1994; Selby et al., 1997). However, a low but detectable amount of the lesion bypass transcript gradually accumulated (Figure 1C, "RO*" in lanes 2–5). The slow rate of the runoff accumulation argued that this product resulted from bypass of the damage site rather than from

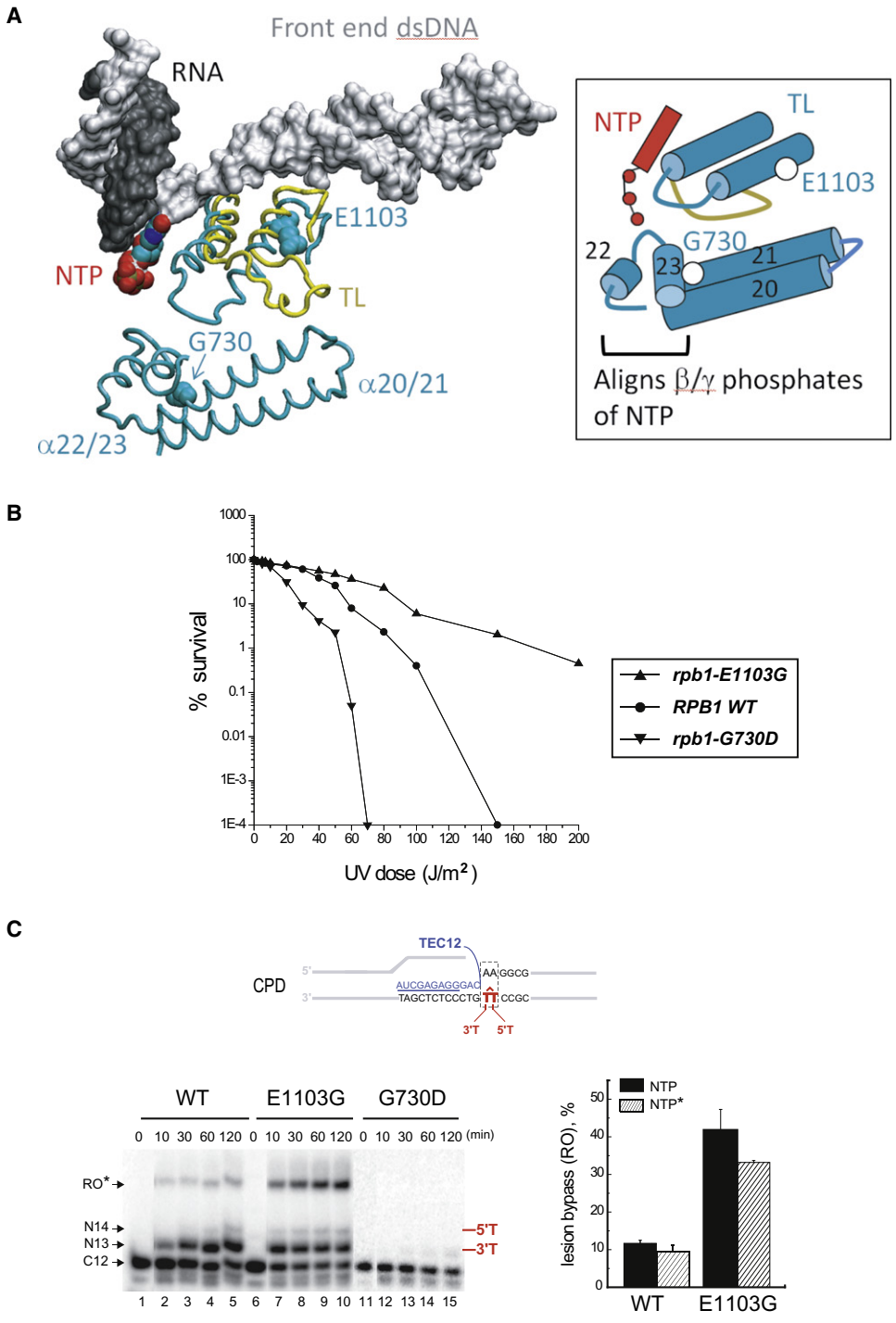

Figure 1. Point Mutations in Pol II Affect Cell Tolerance to UV Irradiation and CPD Bypass In Vitro

(A) TEC structure of *S. cerevisiae* Pol II with the closed (cyan) and the open TL (yellow) (PDB: 2E2H [Wang et al., 2006] and PDB: 1Y1V [Kettenberger et al., 2003]) aligned using the VMD software (Humphrey et al., 1996). The opened TL conformation (in PDB: 1Y1V) structure required the TFIIS protein (not shown). The DNA backbone and RNA are shown in light and dark gray, respectively. Rpb1-E1103 is located at the base of the TL. Rpb1-G730 locates in the α21 helix, the outer region of the secondary channel (Cramer et al., 2001). Cartoon in the box shows contacts of the NTP with the closed TL and α20-α23 helices domain in the secondary channel.

(B) *rpb1-E1103G* mutation increases UV resistance of yeast while *rpb1-G730D* mutation exacerbates the UV sensitivity. Survival was averaged from at least three to five independent experiments.

(C) WT, E1103G, or G730D TEC12 obtained on TT dimer-containing template (TS71-CPD38/NTS71-38) was incubated with NTPs for various times (see Experimental Procedures). The plot shows an average of the results of three experiments and the error bars indicate the standard deviation.

transcription of a residual amount of nondamaged DNA (Figure S1E, lanes 24–29). Thus, Pol II was capable of bypassing a CPD lesion in the transcribed DNA strand, albeit at a dramatically slower rate compared to the CPD in the nontranscribed strand (Figure S1E). The time frame for lesion bypass in vitro is comparable to that of the lesion repair by TC-NER in vivo (Hanawalt and Spivak, 2008).

Importantly, mutations in the catalytic subunit affect the ability of Pol II to transcribe through the lesion in vitro. The Pol II G730D and E1103G error-prone mutant enzymes either abrogated or stimulated the bypass, respectively (Figure 1C, lanes 12–15 and lanes 7–10). E1103G mutant enhanced nucleotide incorporation opposite the 3′T-CPD (compare lanes 2 and 7), which resulted in successful bypass (Supplemental Information and Figure S2). Similarly, glycine substitution of Rpb1 T1095 residue of the TL, which has been implicated in fidelity control by direct interaction with the E1103 residue (Kireeva et al., 2008), also promoted lesion bypass (T1095G, Supplemental Information and Figure S1F). To elucidate the molecular details of the bypass pathway, we carried out a biochemical and a structural characterization of the bypass intermediates.

CPD Does Not Impede Pol II Translocation along DNA

It has been previously proposed that lesions in the template DNA block forward translocation of Pol II causing catalytic arrest (Brueckner et al., 2007). A well described mechanism for arrest of Pol II during transcription is backtracking (Cheung and Cramer, 2011; Komissarova and Kashlev, 1997). The backtracked TEC originates from the pretranslocated state by a one bp backward motion, associated with extrusion of the 3′ end of the RNA into the secondary pore. The pretranslocated TEC contains the 3′ end of the RNA in the NTP-binding site of the active center, thereby preventing loading of the next NTP. The posttranslocated TEC originates from the pretranslocated TEC by a one bp forward movement of the enzyme along RNA and DNA, thereby vacating the NTP-binding site. Binding of the incoming NTP prevents Pol II to return to the pretranslocated state, thus stabilizing the posttranslocated state (reviewed in Burton et al., 2005).

To define the translocation state of the CPD-stalled TEC, we used DNA digestion with exonuclease III (Exo III) (Walmacq et al., 2009). Figure 2 shows the time-resolved rear-end and front-end Exo III footprints of Pol II in TEC12. On the lesion-free template, the pretranslocated state boundary is detected in about half of the TECs after 40 s with Exo III (Figure 2B, lane 2); upon the longer incubation, all convert to the posttranslocated state (lanes 3–5). The presence of a CPD lesion appears to slightly promote forward translocation of Pol II (Figure 2B, compare lanes 3 and 7). The addition of the nonhydrolysable ATP analog shifted the equilibrium toward the posttranslocated state in the regular TEC12 (Figures 2B and 2C; compare lanes 2 and 3 to 11 and 12) but it had little effect on the complex arrested at the lesion, which was already in the posttranslocated state (Figure 2B, compare lanes 7 and 16). Therefore, the CPD lesion may either impair loading of ATP to the active site of posttranslocated Pol II and/or prevent isomerization of the NTP-containing complex into the closed, catalytically competent conformation. This observation is consistent with an extremely low catalytic activity of TEC12 (Figures 1C and S1B).

Probing the front-end boundary in TEC12 with Exo III confirmed that the CPD lesion shifted Pol II to the posttranslocated state (Figure 2E, lanes 2 and 3 and lanes 8 and 9). While the rear-end Exo III footprinting did not show the transient backtracking, the front-end Exo III probing revealed a propensity of Pol II to backtrack. A substantial one bp backtracking was detected on the nonmodified template and on the CPD-containing template (lanes 3–6 and 9–12). The observed difference between the front- and the rear-end footprints of TEC12 is reconciled by the reported ability of Exo III to degrade template DNA upon transient reversible backtracking of RNA polymerase (Kireeva et al., 2008). Notably, the CPD lesion made TEC12 slightly more resistant to backtracking, consequently making the front-end DNA more resistant to Exo III (lanes 3 and 4 and lanes 9 and 10 and Figure 2F). Thus, Pol II is stabilized in the posttranslocated state by the downstream CPD, ruling out the possibility of backtracking as the mechanism of stalling by CPD.

Nontemplated AMP Incorporation Opposite the 3′T-CPD According to the A-Rule

Similarly to Pol II stalling at *cis-platin* damaged DNA, the prolonged pausing at a 3′T-CPD may also result from impaired entry of the CPD into the polymerase active site. Such impairment was shown to promote nontemplated RNA synthesis across *cis-platin* damaged DNA (Damsma et al., 2007). To identify the source of CPD-induced pausing, we compared the selectivity of nucleotide incorporation during transcription of templates containing the CPD or an abasic site replacing the 3′T-CPD (Figures 3A and 3B). The RNA products of the same length but carrying the different 3′ terminal NMPs have different electrophoretic mobilities in the gel allowing distinction between the proper ATP incorporation and the misincorporation (Kireeva et al., 2008). Notably, the effects of both lesions on the first NTP incorporation were strikingly similar. Incubation of TEC12 with individual NTPs revealed that Pol II selectively incorporated AMP opposite the 3′T-CPD and the 3′ abasic site. For both lesions, incubation with 1 mM ATP resulted in RNA extension by three nucleotides, while in the presence of all four NTPs extension was limited to one nucleotide (Figures 3A, lanes 14 and 7, and 3B, lanes 9 and 5). In both cases, Pol II incorporated A13 to the RNA opposite the 3′T-CPD or the abasic site. However, in the presence of ATP only, the A13 product was slowly extended to A14 and A15 products (Figure 3A, lanes 9–14, and 3B, lanes 6–9). The A15 product resulted from misincorporation of AMP (for GMP) one bp beyond the lesion (Figures 3A, lane 14, and 3B, lane 9). RNA extension beyond position A13 was strongly inhibited in the presence of four NTPs. Importantly, the nontemplated AMP incorporation opposite the abasic site appears to be crucial for lesion bypass by Pol II. AMP incorporation opposite the 3′T-CPD is also likely to be nontemplated. Upon the prolonged incubation with ATP followed by a short chase with four NTPs, the A14 product was quantitatively elongated to the run-off product (Figures 3A, lane 15, and 3B, lane 10). Thus, we conclude that the lesion bypass pathway involves AMP incorporation opposite both thymines of the CPD. This result is consistent with the lesion bypass observed when a TEC was

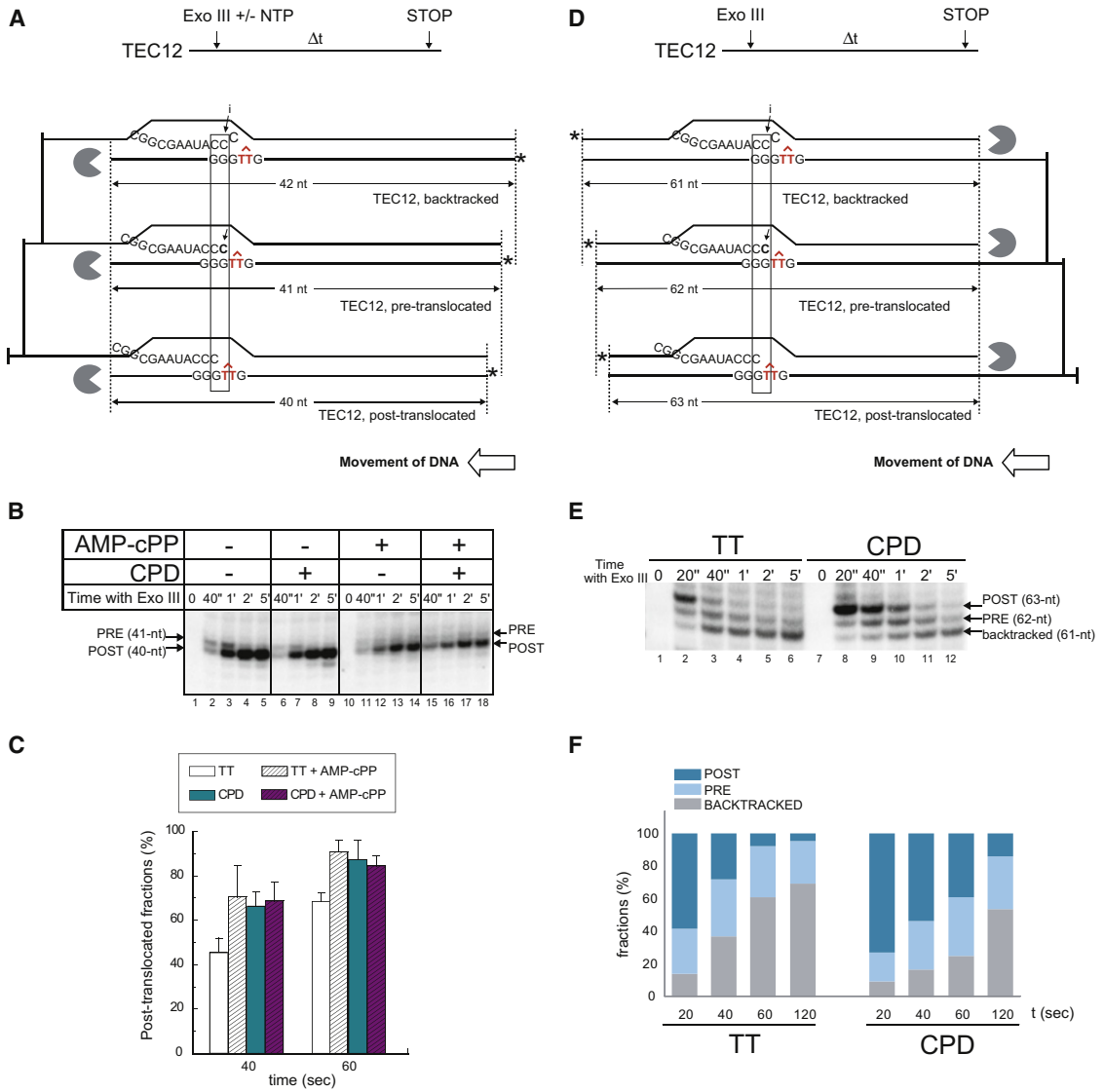

Figure 2. A CPD Lesion Stabilizes the TEC in the Posttranslocated States

(A) Rear-end footprint experimental setup. The figure illustrates the predicted translocation register of lesion-stalled TECs. The length of the template DNA strand protected from Exo III digestion differs by one nucleotide between the backtracked (42 nt), the pretranslocated (41 nt) and the posttranslocated (40 nt) state of TEC12.

(B) Dynamics of DNA degradation by Exo III revealed equilibrium between pre- and posttranslocated states of the TEC.

(C) The lesion confers a shift of the equilibrium toward the posttranslocated state, but inhibits stabilization of the posttranslocated state of Pol II by an incoming NTP. The quantification was based on the results of at least three separate experiments and the error bars show the standard deviation.

(D) Front-end footprint experimental setup.

(E) Mapping of the translocation register of Pol II front-end boundary revealed that the lesion does not promote backtracking of TEC12.

(F) The bottom panel depicts the distribution of the three distinct front-end boundaries detected in TEC12 at various incubation times with Exo III.

assembled directly at the CPD site with the RNA primer carrying two adenines complementary to the thymine bases of the CPD (Brueckner et al., 2007).

Under physiological conditions, the translesion synthesis across the 3′T-CPD as well as the abasic site is inhibited by competition between ATP and the other NTPs (Figures 3A, compare lanes 2 and 9, and 3B, lanes 2 and 6). Despite this competition, no significant misincorporation at the 3′T-CPD occurred whereas incubation with either UTP, CTP, or GTP alone resulted in significant misincorporation opposite the 3′T-CPD (Figure 3A, lanes 14, 21, 28, and 35) or the abasic site (Figure 3B, lanes 9, 14, 19, and 24) with rates within the same range as that of ATP (Figure 3C). Importantly, this misincorporation at the 3′T prevents subsequent ATP incorporation opposite the 5′T and eliminates the bypass on subsequent incubation with all four NTPs (lanes 15, 22, 29, 36). These data were consistent with

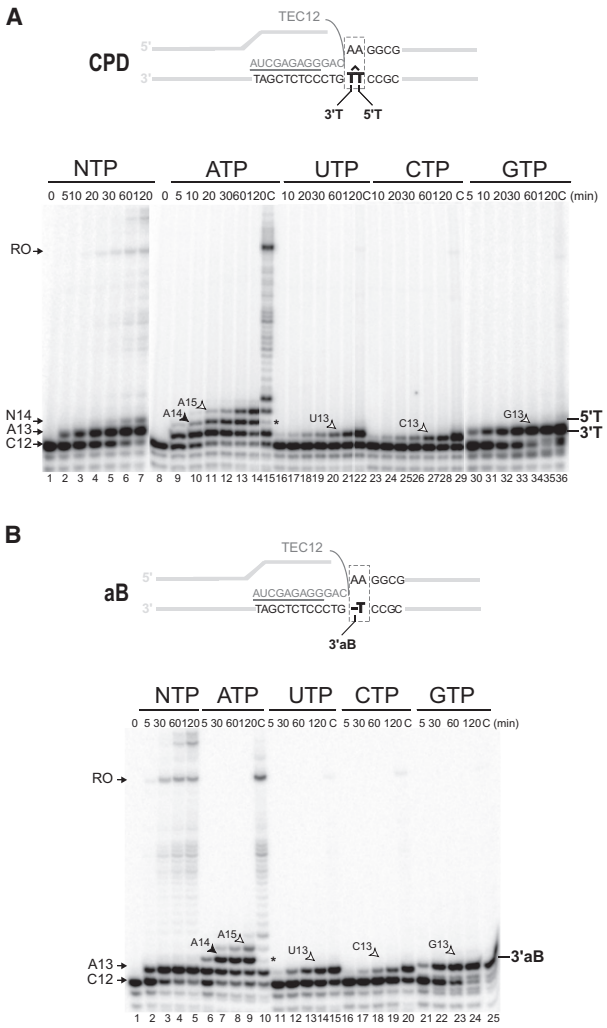

C

	TT k_{app} (s^{-1})	CPD k_{app} (s^{-1})	aB k_{app} (s^{-1})
ATP	20 ± 3	(26.5 ± 0.5)x10^{-4}	(37.1 ± 1.7)x10^{-4}
UTP	(3.2 ± 0.5)x10^{-4}	(0.7 ± 0.1)x10^{-4}	(1.2 ± 0.2)x10^{-4}
CTP	(1.7 ± 0.3)x10^{-4}	(0.9 ± 0.1)x10^{-4}	(1 ± 0.2)x10^{-4}
GTP	(8.1 ± 0.3)x10^{-4}	(5.4 ± 0.4)x10^{-4}	(2.6 ± 0.7)x10^{-4}

Figure 3. Pol II Employs the A-Rule to Conduct ATP Insertion Opposite the 3′T-CPD

(A) Preferential AMP incorporation opposite the 3′T-CPD. TEC12 was obtained from TEC9 on CPD-DNA as described in Figure 1C and incubated with 1 mM individual NTP or four NTPs for different times. Individual NTP reactions were subsequently chased with four NTPs for 15 min (C). Black and white arrows indicate normal incorporation products and misincorporation, respectively. The longer RNA A15 derived from AMP incorporation opposite both thymines followed by misincorporation of A for G.

(B) Nontemplated AMP incorporation opposite an abasic site (3′aB).

(C) Apparent rate constants of the correct and incorrect NTP incorporation on regular, CPD, and aB DNA. The data shown are an average of three parallels and the error values were obtained from the single-exponential fit of the data.

the previous sequencing analysis of CPD-arrested transcripts showing that Pol II was irreversibly stalled after incorporating an incorrect nucleotide opposite the lesion (Mei Kwei et al., 2004).

A quantitative analysis demonstrated that the efficiency of nontemplated AMP incorporation opposite an abasic site was comparable to that opposite the 3′T-CPD (Figure 3C). On the regular template, the cognate AMP incorporation opposite T occurs at a rate of 20 s^{-1}; the rate of AMP incorporation opposite the 3′T-CPD or the abasic site is four orders of magnitude lower (Figure 3C). In contrast, the impact of the abasic site and CPD on the noncognate nucleotide misincorporation is much more subtle: the misincorporation rates are decreased only about 3-fold on the lesion-containing templates compared to the unmodified template. This result suggests that the incorporation of UMP, CMP, and GMP opposite the 3′T occurs by a mechanism similar to misincorporation on a normal DNA (Walmacq et al., 2009). Importantly, Pol II preferentially incorporates AMP, and to a lesser extent GMP, opposite the 3′T-CPD or an abasic position. Such preferential, nontemplated AMP incorporation was previously described for replicative DNA polymerases that encounter a bulky DNA lesion and is known as the A-rule (Strauss, 1991; Taylor, 2002). Together, these observations demonstrate that Pol II is able to initiate TLS by nontemplated AMP incorporation according to the A-rule. This mechanism is consistent with the model where the CPD lesion does not enter the active site during nucleotide insertion opposite the 3′T-CPD (Brueckner et al., 2007; Damsma et al., 2007).

Misincorporation at the 5′T Abrogates CPD Bypass

In the presence of ATP, lesion bypass was completed after Pol II slowly incorporated AMP (A14) opposite the 5′T-CPD (Figures 3A, lane 14, and 3B, lane 9). This product was rapidly extended to the run-off product by subsequent incubation with four NTPs (Figures 3A, lane 15, and 3B, lane 10). However, with all NTPs, accumulation of a nonextendable 14 nt product having a distinct mobility from the A14 RNA became apparent indicating a NTP misincorporation event (Figure 3A, lane 7). To identify the source of this misincorporation, we analyzed RNA extension by TEC13A (Figure 4). Prolonged incubation of TEC13A with ATP alone followed by chase with four NTPs caused accumulation of a significant lesion bypass product (Figure 4, compare lanes 8–10), whereas immediate incubation of TEC13A with four NTPs resulted in weaker bypass (~7%–10%) (Figure 4, lane 7). This result is similar to the pattern obtained with TEC12 (Figure 3A, lane 7); it suggests that the noncomplementary NTPs compete with ATP for the incorporation opposite the 5′T of the lesion similarly to the competition observed at the 3′T position. Testing incorporation of each NTP revealed that UMP, but not CMP or GMP, is incorporated in TEC13. Unlike A14 incorporation, UMP misincorporation completely abrogated the bypass (Figure 4A, lanes 11–13). Notably, upon incubation of TEC13 with all four NTPs, the UMP misincorporation at the 5′T represented the major event, and it constituted the main cause of arrest at the lesion (Figure 4A, lane 7). This finding was consistent with previous results (Brueckner et al., 2007). Importantly, the rule driving nucleotide incorporation opposite the 5′T differs from the significantly more selective nontemplated AMP

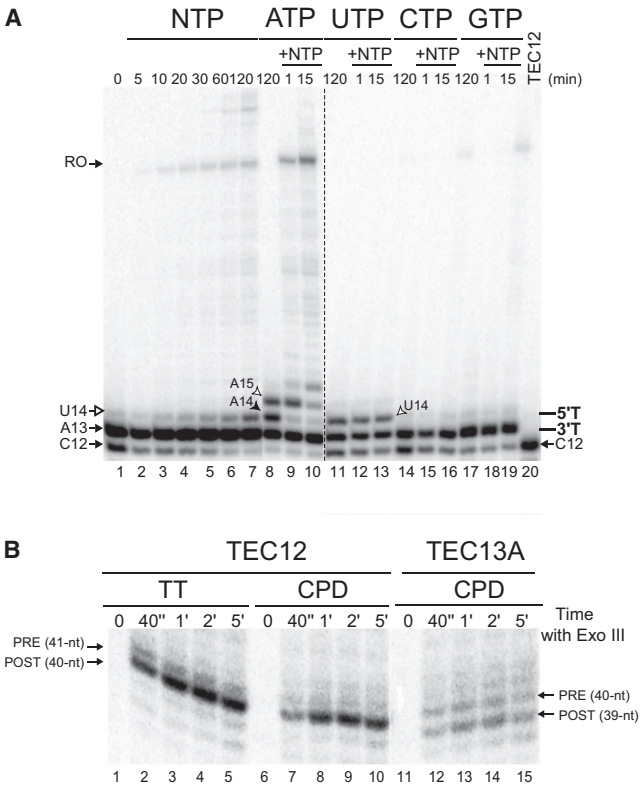

Figure 4. UTP Misincorporation Opposite the 5′T-CPD Abrogates Lesion Bypass

(A) TEC13A obtained from TEC12 was incubated with 1 mM individual NTP for 120 min or four NTPs for indicated time. Individual NTP reactions were subsequently chased with four NTPs. AMP incorporation opposite the 5′T is required for lesion bypass while UMP misincorporation results in irreversible stalling.

(B) Rear-end Exo III footprinting of TEC13A obtained from TEC12 as described in Figure 2B.

incorporation at the 3′T. For the 5′T, Pol II showed a strong discrimination against CTP and GTP and less for ATP and UTP, indicating that this reaction may be partially directed by the 5′T base in the template. Indeed, the Exo III footprinting of TEC13 revealed the equilibrium between the pretranslocated and posttranslocated states, indicating successful loading of the 5′T to the active center (Figure 4B, lane 12). We conclude that Pol II negotiation with the CPD lesion results in the nontemplated AMP incorporation according to the A-rule followed by either an addition of another AMP leading to lesion bypass or a misincorporation of UMP leading to arrest (Figure 6).

Structural Basis for CPD Translocation and Nontemplated Incorporation

Previous work provided the structures of Pol II TECs with a CPD lesion in the downstream DNA (positions i+2/i+3) and within the active center (positions i, i+1) (Brueckner et al., 2007). Here we provide the missing crystal structure of the intermediary state with the CPD in position i+1/i+2, which shows how the lesion can be translocated into the active center and indicates the structural basis for nontemplated AMP incorporation at a lesion (Figures 3 and 4). The crystal structure of this CPD-TEC stalled at the 3′T of the lesion was solved and the nucleic acid sequence within the complex was unambiguously assigned by anomalous scattering from a bromo-uracil marker in the template strand (Figure 5A, intermediate state). This TEC was crystallized with DNA/RNA sequences that differ to the TEC12 scaffold, in order to optimize crystallization and diffraction properties (Table 1).

In the new structure, the CPD-TEC adopts the posttranslocated conformation with the 3′ end of the nascent RNA adjacent to an open NTP-binding site (Figure 5A, intermediate state). In contrast to a nondamaged posttranslocated complex (Kettenberger et al., 2004; Westover et al., 2004), which has the template DNA i+1 base positioned for hybridization with the incoming NTP next to the bridge helix in the active site, the corresponding i+1 base is part of a CPD that is positioned above the bridge helix, and the normal site for the templating DNA base is unoccupied. This impaired loading of the CPD in the active site results in the relaxed conformation of the catalytic pocket, causing an extra space for the accommodation of incoming NTPs without the constraints normally imposed by the pairing template base (i+1) in the TEC (Figure 5B, structures II and III). In the regular posttranslocated TEC, the 3′ end of the transcript is base-paired with its complementary DNA base in position i of the template strand (Figure 5B, left side bottom section). In the CPD-TEC, the i template base is dislodged from its normal location and does not pair with the 3′ end of the RNA, but rather stacks opposite the 3′T-CPD (Figure 5B, left side top section). The lack of a templating base in the active site provides sufficient space to accommodate a bulky purine residue (ATP or GTP) in the active center. These results are consistent with the model that translesion transcription involves a nontemplated NTP addition opposite the 3′T of the CPD located above the bridge helix in an intermediary state of translocating the lesion into the active site.

Role of Translesion Transcription in Transcription-Coupled NER (TC-NER)

The inactivation of GG-NER (*rad16*) showed a differential UV resistance for the *rpb1-E1103G* and *rpb1-G730D* cells indicating that an efficient TLS positively correlated with UV cell survival (Figure 1B). Note that the TC-NER, involving recruitment of the repair proteins to the CPD-stalled Pol II by Rad26, remained active in the *rad16* cells (Li and Smerdon, 2004). To address whether the TLS contribution to UV survival required TC-NER, we generated a deletion of the *RAD26* gene in the cells harboring Pol II mutations (see Supplemental Experimental Procedures). The graph in Figure 5C showed that inactivation of TC-NER (*rad26*) alone rendered *rpb1-G730D* cells partially UV-sensitive with no detectable effect on the WT *RPB1* cells (van Gool et al., 1994). The subsequent inactivation of GG-NER (*rad16rad26*) made these cells hypersensitive to UV light. In contrast, inactivation of TC-NER (*rad26*) had no effect on the TLS-proficient *rpb1-E1103G* mutant unless *RAD16*-mediated GG-NER was additionally eliminated. Importantly, the *RAD26* deletion (with *RAD16* deletion) completely abolished the positive contribution of *rpb1-E1103G* mutation to the UV survival ultimately linking TLS to TC-NER. This conclusion was consistent

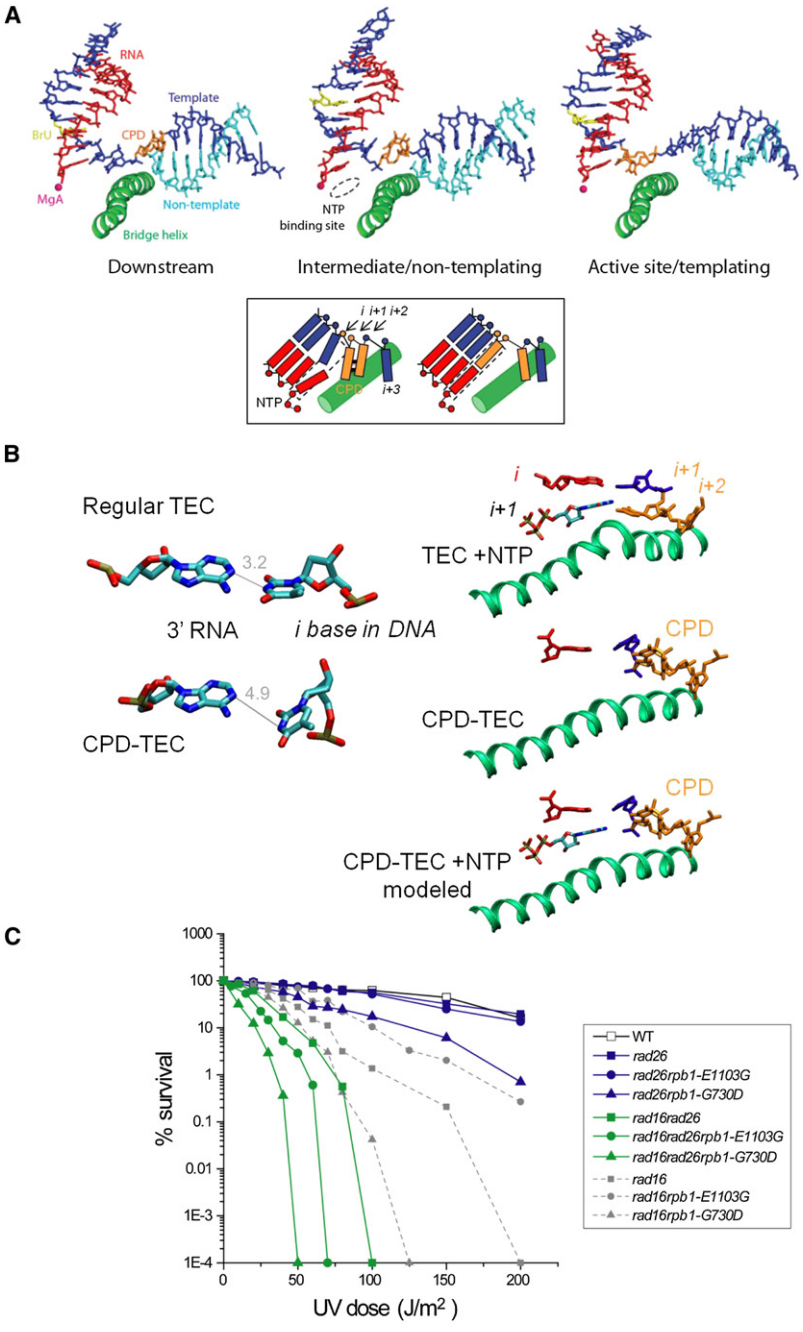

Figure 5. Crystal Structure of TEC Stalled at the CPD Reveals Foundation for the A-Rule

(A) A wire-frame representation of the crystal structure of the CPD lesion-containing TEC9 stalled upstream the CPD (positions i+1/i+2). Pol II TEC structures with a CPD lesion located in the downstream DNA (positions i+2/i+3) and within the active center (positions i/i+1) are also shown (Brueckner et al., 2007). The RNA, template, and non-template DNA are highlighted in red, dark blue, and cyan, respectively. The bridge helix (BH) is shown in green. The cartoons on the bottom highlight the details of the structure on the TT regular (right) and CPD-containing DNA (left).

(B) The details of the configuration of the RNA 3′ end in the regular posttranslocated TEC (PDB: 2E2H) and in its CPD-stalled counterpart from (A). The numbers represent the distances in angstroms between the 3′ purine base and the complementary pyrimidine in the template DNA. The structures on the right display a conformation of the BH and the *i*+1/*i*+2 DNA bases in the regular posttranslocated TEC with the incoming NTP (I), the CPD-TEC without NTP (II), and in the CPD-TEC with the modeled purine nucleotide in the active center (the NTP coordinates taken from PDB: 2E2H).

(C) Pol II activity modulates UV resistance by *RAD26*-dependent and *RAD26*-independent pathways. Yeast strains carrying *RPB1WT* (square), *rpb1-E1103G* (circle), or *rpb1-G730D* (triangle) mutation in the *rad16rad26* and *rad26* background were irradiated with increasing UV doses. UV sensitivity of yeast cells in the isogenic *rad16* background was also measured independently from Figure 1B (see Supplemental Information).

DISCUSSION

We provide biochemical and crystallographic evidence for the mechanism of lesion bypass by Pol II and its possible role in cellular resistance to UV-induced DNA damage. As depicted in Figure 6, TLS occurs by a nontemplated insertion of AMP opposite the 3′T-CPD following the A-rule (steps 1→2→3), followed by a templated AMP insertion opposite the 5′T-CPD (step 4→5b). During the nontemplated AMP insertion, the CPD moiety is placed over the bridge helix (step 2→3). The CPD then translocates into the polymerase active center (step 3→4), and the 5′T-CPD then directs slow incorporation of a cognate AMP (step 4→5b) (Brueckner et al., 2007). Translocation is disfavored as previously reported (Brueckner et al., 2007), but our DNA footprinting data showed that it is not totally blocked. The nontemplated incorporation of the first AMP may help to stabilize the next state in TLS with the CPD translocated into the active site by pairing of the 3′AMP with the 3′T-CPD (step 3→4). Accommodation of the CPD within the active site is probably accompanied by conformational changes, such as TL opening and BH straightening, to poise the complex for the next cycle of NMP (AMP) addition. Once the CPD is in the active site and both AMPs are incorporated, Pol II can easily complete the

with the enhanced UV sensitivity of the TLS-deficient *rpb1-G730D* mutant in both *rad16rad26* and *rad26* background. In summary, both *rpb1-E1103G* and *rpb1-G730D* mutations rely on the Rad26 component of TC-NER to tolerate the DNA damage. This effect may include removal of CPD-stalled Pol II molecules from DNA as an alternative to their degradation, which results in restoration of transcription and replication of the damaged DNA in addition to exposing the lesions to TC-NER and GG-NER proteins as previously suggested (Hanawalt and Spivak, 2008).

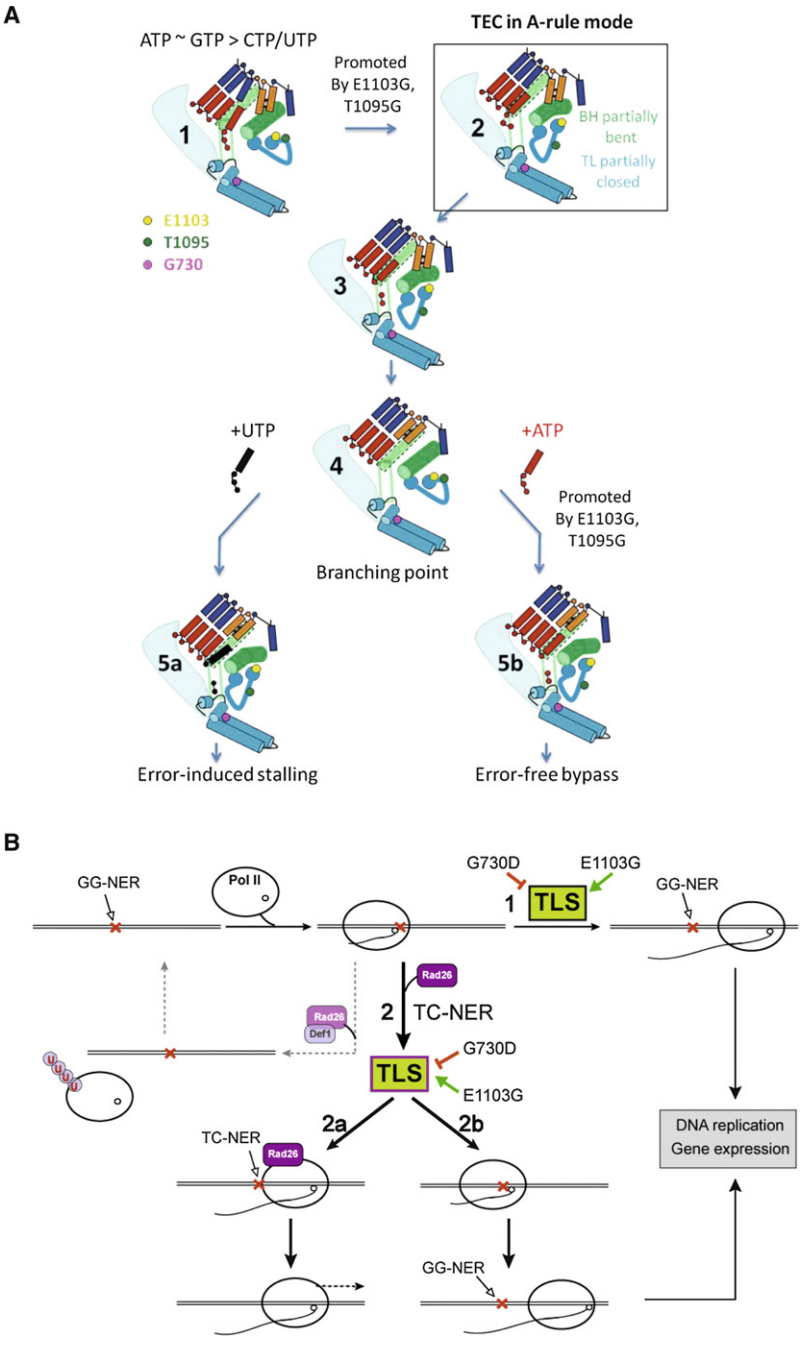

Figure 6. Steps in the CPD Bypass

(A) Individual steps in negotiation of Pol II with a CPD lesion (orange) and putative conformational changes in the TL (cyan) and the BH (green) leading to the error-free bypass or irreversible stalling. The NTP binding site (*i*+1 site) is shown in light green. An interaction between Rpb1-E1103 (yellow) and T1095 (green) residues of the TL during the lesion bypass is shown. G730D mutation (magenta) affects the proper alignment of the 4-helix α20–α23 domain (cyan cylinders) of Rpb1 subunit in the secondary channel with the incoming NTP (red).

(B) The proposed connection between GG-NER, TC-NER, and TLS pathways in cellular resistance to UV-induced DNA damage. Encounter with a CPD lesion results in Pol II stalling at the damage site (red 'X'). The numbers mark: (1) Rad26-independent TLS followed by repair by GG-NER (2) initiation of TC-NER by Rad26 (in purple) recruitment to the CPD-stalled Pol II followed by (2a) the induction of TLS to expose the CPD to TC-NER, (2b) GG-NER, or resumption of transcription without repair (not shown). The dashed lane represents a pathway alternative to TLS, which involves Pol II ubiquitination and degradation after recruitment of Rad26/Def1 complex. TLS may contribute to UV cellular resistance by preventing collisions between both replication and transcription machineries. E1103G and G730D Pol II mutations promote and inhibit (1) and (2) TLS, respectively.

CPD bypass. Apparently, the CPD is translocated through the RNA-DNA hybrid without major restraints.

The observed differences in nucleotide selectivity opposite the two thymines of the CPD further support the proposed mechanism for lesion bypass. During insertion opposite the 3′T, the incorporation of AMP is favored 5-fold over the insertion of GMP, which is comparable to the nucleotide incorporation tendency opposite an abasic site. This preferential adenine insertion is strikingly similar to the A-rule proposed for DNA polymerases (Obeid et al., 2010; Strauss, 1991). The nucleotide insertion opposite the 5′T exhibits a much greater selectivity for ATP over GTP or CTP, but a poor discrimination against UTP, likely reflecting the base-pairing abilities of the 5′T of the CPD with an incoming ATP. The strong discrimination against GTP may be dictated by a failure to accommodate a bulky GTP:5′T mismatch in the constrained active site already occupied by the bulky CPD. The strong selection against the CTP:5′T mismatch may reflect the reported intrinsic property of Pol II to misincorporate UMP better than CMP opposite nonmodified thymines in DNA (Kireeva et al., 2008). It is also possible that a UTP 5′T wobble bp is formed in the active site, promoting UMP misincorporation (Brueckner et al., 2007). The posttranslocated TEC appears to be a mechanistic branch-point between two pathways, error-induced stalling or error-free bypass. The first pathway involving UMP misincorporation opposite the 5′T results in irreversible stalling of Pol II (step 4→5a), in good agreement with previous studies (Brueckner et al., 2007). The alternative pathway, which only occurs when AMP is incorporated opposite both thymines, enables lesion bypass (step 4→5b).

The different aspects of translesion transcription emphasize the striking similarities of Pol II with both replicative and translesion DNA polymerases (Figure S3). Similar to the replicative polymerases, Pol II excludes the CPD from its active site and catalyzes the nontemplated insertion opposite the 3′T-CPD. The template-independent mechanism may be similar to the

Table 1. Data Collection and Refinement Statistics

Data Collection Statistics	
Space group	C 2 2 2_1
Unit cell axes (Å)	221.64, 391.52, 281.77
Wavelength (Å)	0.9188
Resolution range (Å)	56.2 - 3.40 (3.58 - 3.40)
No. unique reflections	167266 (24255)
Completeness	100 (100)
Redundancy	7.0 (6.6)
Mosaicity (°)	0.34
Rsym	0.118 (0.787)
I/σ(I)	10.7 (2.3)
Refinement Statistics	
Non H atoms	32125
RMSD bonds (Å)	0.011
RMSD angles (°)	1.498
Rcryst	0.165
Rfree	0.199
Molprobity Ramachandran Plot	
% Residues in preferred/ allowed/disallowed regions	88.6/8.4/3.1

Values in parenthesis are for the highest resolution shell.

one reported for the DNA polymerase KlenTaq where a tyrosine side chain of the O-helix (a functional homolog of the bridge helix) enters an empty active site and participates in formation of a selective hydrogen bond with the incoming ATP to mimic its pairing with the template thymine, which is flipped out of the active site as a part of the CPD lesion (Obeid et al., 2010). On the other hand, Pol II accommodates the CPD in the active site after the first AMP insertion to promote the second AMP addition, which completes the lesion bypass similar to translesion DNA polymerases. The switch between these two modes may involve *cis*-acting Pol II domains such as the trigger loop and bridge helix, and *trans*-acting regulatory factors that might promote lesion bypass in vivo (Charlet-Berguerand et al., 2006). The mutations altering transcription fidelity are proposed to modulate the CPD bypass by affecting the flexibility of the Pol II active center. The lack of correlation between the miscoding potential of a given lesion and the efficiency of its bypass was previously reported for Pol II (Charlet-Berguerand et al., 2006) and translesion DNA polymerases (Waters et al., 2009). Rpb1-E1103G and T1095G mutations promote the nucleotide insertion opposite both thymines of the CPD (Figures 6, steps 1→3 and 4→5b, S1C, and S2). Both AMP insertions are possibly stimulated by a partial TL closure on the substrate within the disturbed active center, thus preventing rapid ATP dissociation before bond formation (Kaplan et al., 2008; Kireeva et al., 2008). In addition, TL movement might affect bending of the bridge helix involved in forward translocation of Pol II (Kireeva et al., 2010). Therefore, E1103G and T1095G mutations may promote the second AMP insertion by facilitating delivery of both thymines within the active site through a stronger kinking of the bridge helix (step 3→4). As a result, both mutants transcribe across the CPD lesion with a relatively high efficiency. Interestingly, E1103G stimulates misincorporation of UMP opposite thymine on regular DNA (Kireeva et al., 2008) but not opposite the 5′T-CPD (Figure S2B). The bulky 5′T-CPD:U mismatch in the active center may more strongly interfere with the trigger loop closure than the compact T:U mismatch, thus overcoming the stimulation of UMP misincorporation by the E1103G mutant.

The successful lesion bypass observed with Rpb1-E1103G Pol II in vitro correlates with an increased cell survival upon UV irradiation, but only in the absence of *RAD16*-dependent GG-NER. In contrast, G730D mutation, which abrogates bypass in vitro, consistently increases the UV sensitivity of *RAD16*-deficient yeast cells (Figure 1B). Importantly, the increased UV resistance of the *rpb1-E1103G* mutant required the functional *RAD26* gene involved in TC-NER initiation, ultimately linking the translesion transcription to TC-NER (Figure 5C). We argued that the facilitated clearance of the lesion by the E1103G-Pol II serves to expose the lesions to the TC-NER proteins after their Rad26-dependent recruitment to the CPD-stalled Pol II (Figure 6B, pathway 2a). This mechanism may be essential for TC-NER as an alternative to removal of Pol II from the lesion by ubiquitin-dependent degradation (Woudstra et al., 2002) and to the proposed excision of the damaged DNA strand together with the Pol II arrested on the lesion (Brueckner et al., 2007).

Interestingly, *RAD26*-mediated TC-NER contributed to the UV resistance of the TLS-deficient *rpb1-G730D* cells even in the presence of the fully active *RAD16*-mediated GG-NER (Figure 5C). We argued that the presence of many CPD-arrested Pol II sensitize the cells to UV light, making TC-NER essential for the repair or exposure of these lesions to the GG-NER (Figure 6B). Indeed, the inactivation of GG-NER in these cells rendered them hypersensitive to UV irradiation (Figure 5C). In addition, TC-NER might contribute to UV survival of the TLS-deficient cells by removal of the CPD-arrested Pol II from the genes independently or coincidentally with DNA repair. Moreover, TLS might allow unimpeded replication of the damaged DNA and completion of the ongoing rounds of mRNA production in the irradiated cell to provide a steady supply of the housekeeping and repair proteins under persistence of the bulky lesions in transcribed genes. Both damage tolerance mechanisms should prevent the lethal consequences of unrepaired lesions in DNA (Figure 6B). The increased UV resistance rendered by *rpb1-E1103G* and *rpb1-T1095G* mutations may reduce the risk of collision between the replication fork and CPD-arrested Pol II. These collisions lead to double-strand DNA breaks, genomic instability, and cell death (Pomerantz and O'Donnell, 2010). Taken together, these observations support earlier suggestions that the enhanced UV sensitivity may be in part a consequence of arrested transcription rather than a defect in DNA repair (Friedberg, 1996).

Unfaithful transcription through damaged DNA has been proposed to contribute to mutagenesis and to the initiation and progression of human diseases (Saxowsky and Doetsch, 2006). The error avoidance mechanism enabling Pol II to faithfully transcribe through the CPD lesion by implementation of the A-rule limits transcriptional mutagenesis. It remains to

be established whether the A-rule is universal for transcription across other types of DNA lesions. Future studies should focus on the TLS role in transcription-coupled DNA repair and on identification of Pol II partners regulating CPD bypass in vivo.

EXPERIMENTAL PROCEDURES

Media, Yeast Manipulations, and Strains

Media, growth conditions, and yeast manipulations as well as any associated references are described in Supplemental Information.

Analysis of Sensitivity to UV

Yeast cells were grown in YEPD at 28°C to mid-log phase (optical density at 600 nm of ~1.0), diluted in water, and plated in triplicate on YEPD plates. The plates were immediately irradiated with a Stratalinker UV crosslinker (Stratagene) at the indicated doses of UV. After 2–3 days of incubation at 28°C in the dark, colonies were counted, and survival was calculated as described (van Gool et al., 1994).

Enzymes, Oligonucleotides, and Reagents

RNA, unmodified DNA oligonucleotides, and abasic site template DNA (Table S1) were from IDT (San Diego, CA). *Cis-syn* Thymine Dimer Phosphoramidite (50 μM) was purchased from Glen Research (Sterling, VA). The CPD-containing DNA oligonucleotides were synthesized and purified by PAGE electrophoresis by Oligos Etc. (Wilsonville, OR). NTPs were from GE Healthcare (Piscataway, NJ) and 3′dNTPs from Invitrogen. Exonuclease III was from New England Biolabs (Bedford, MA). WT Pol II, Rpb1-E1103G, Rpb1-G730D, and Rpb1-T1095G were obtained and purified as described previously (Kireeva et al., 2008).

TEC Assembly and In Vitro Transcription Assays

Full methods for TEC assembly and in vitro translesion assays are detailed in Supplemental Information. To facilitate detection of full-length lesion bypass product (RO, 51 nt) obtained under the standard NTP chase conditions (ACGU, 1 mM), CPD-containing TEC12s were also incubated with a mixture of NTP* containing a terminator chain NTP (AGU, 1 mM; 3′dCTP, 100 μM) which generates a shorter lesion bypass product (RO*, 15 nt) (Figure 1C). The quantitative results represent averages of three independent experiments with error bars showing standard deviation (Figure 1C, graph).

Exonuclease III Footprinting

TEC12s were assembled with the wild-type enzyme with RNA7 on lesion-free template (TS71-25) or lesion-containing template DNA (TS71-CPD25) with the fully complementary NTS71-25E (rear-end footprinting) or NTS71-25E2 (front-end footprinting). Where indicated, 1 mM nonhydrolysable AMP-cPP was added. The footprinting reactions were done and analyzed as described (Walmacq et al., 2009).

Crystal Structure Analysis

Full methods for *Saccharomyces cerevisiae* 12-subunit Pol II purification, crystallization, and structure determination as well as any associated references are described in Supplemental Information.

ACCESSION NUMBERS

Protein Data Bank: Coordinates and structure factors of the complete CPD-stalled Pol II complex crystal structure have been deposited under accession code 4A93.

SUPPLEMENTAL INFORMATION

Supplemental Information includes Supplemental Text, three figures, two tables, Supplemental Experimental Procedures, and Supplemental References and can be found with this article online at doi:10.1016/j.molcel.2012.02.006.

ACKNOWLEDGMENTS

We thank Brenda Schafer for technical help and Alison Rattray and Donald Court for helpful discussion and for critical reading of the manuscript. This research was supported by the Intramural Research Program of the National Institutes of Health, National Cancer Institute. The contents of this publication do not necessarily reveal the views of the policy of the Department of Health and Human Services, nor does mention of trade names, commercial products, or organizations imply endorsement by the U.S. government. Part of this work was performed at the Swiss Light Source at the Paul Scherrer Institut, Villigen, Switzerland. P.C. was supported by the Deutsche Forschungsgemeinschaft, SFB646, TR5, FOR1068, NIM, Bioimaging Network BIN, and the Jung-Stiftung.

Received: April 29, 2011
Revised: November 28, 2011
Accepted: February 10, 2012
Published online: March 8, 2012

REFERENCES

Bohr, V.A., Smith, C.A., Okumoto, D.S., and Hanawalt, P.C. (1985). DNA repair in an active gene: removal of pyrimidine dimers from the DHFR gene of CHO cells is much more efficient than in the genome overall. Cell *40*, 359–369.

Brooks, P.J., Wise, D.S., Berry, D.A., Kosmoski, J.V., Smerdon, M.J., Somers, R.L., Mackie, H., Spoonde, A.Y., Ackerman, E.J., Coleman, K., et al. (2000). The oxidative DNA lesion 8,5′-(S)-cyclo-2′-deoxyadenosine is repaired by the nucleotide excision repair pathway and blocks gene expression in mammalian cells. J. Biol. Chem. *275*, 22355–22362.

Brueckner, F., Hennecke, U., Carell, T., and Cramer, P. (2007). CPD damage recognition by transcribing RNA polymerase II. Science *315*, 859–862.

Burton, Z.F., Feig, M., Gong, X.Q., Zhang, C., Nedialkov, Y.A., and Xiong, Y. (2005). NTP-driven translocation and regulation of downstream template opening by multi-subunit RNA polymerases. Biochem. Cell Biol. *83*, 486–496.

Charlet-Berguerand, N., Feuerhahn, S., Kong, S.E., Ziserman, H., Conaway, J.W., Conaway, R., and Egly, J.M. (2006). RNA polymerase II bypass of oxidative DNA damage is regulated by transcription elongation factors. EMBO J. *25*, 5481–5491.

Cheung, A.C., and Cramer, P. (2011). Structural basis of RNA polymerase II backtracking, arrest and reactivation. Nature *471*, 249–253.

Cramer, P., Bushnell, D.A., and Kornberg, R.D. (2001). Structural basis of transcription: RNA polymerase II at 2.8 angstrom resolution. Science *292*, 1863–1876.

Damsma, G.E., and Cramer, P. (2009). Molecular basis of transcriptional mutagenesis at 8-oxoguanine. J. Biol. Chem. *284*, 31658–31663.

Damsma, G.E., Alt, A., Brueckner, F., Carell, T., and Cramer, P. (2007). Mechanism of transcriptional stalling at cisplatin-damaged DNA. Nat. Struct. Mol. Biol. *14*, 1127–1133.

Donahue, B.A., Yin, S., Taylor, J.S., Reines, D., and Hanawalt, P.C. (1994). Transcript cleavage by RNA polymerase II arrested by a cyclobutane pyrimidine dimer in the DNA template. Proc. Natl. Acad. Sci. USA *91*, 8502–8506.

Friedberg, E.C. (1996). Relationships between DNA repair and transcription. Annu. Rev. Biochem. *65*, 15–42.

Hanawalt, P.C., and Spivak, G. (2008). Transcription-coupled DNA repair: two decades of progress and surprises. Nat. Rev. Mol. Cell Biol. *9*, 958–970.

Hoeijmakers, J.H. (2001). Genome maintenance mechanisms for preventing cancer. Nature *411*, 366–374.

Humphrey, W., Dalke, A., and Schulten, K. (1996). VMD: visual molecular dynamics. J. Mol. Graph. *14*, 33–38, 27–28.

Kaplan, C.D., Larsson, K.M., and Kornberg, R.D. (2008). The RNA polymerase II trigger loop functions in substrate selection and is directly targeted by alpha-amanitin. Mol. Cell *30*, 547–556.

Kettenberger, H., Armache, K.J., and Cramer, P. (2003). Architecture of the RNA polymerase II-TFIIS complex and implications for mRNA cleavage. Cell *114*, 347–357.

Kettenberger, H., Armache, K.J., and Cramer, P. (2004). Complete RNA polymerase II elongation complex structure and its interactions with NTP and TFIIS. Mol. Cell *16*, 955–965.

Kireeva, M.L., Nedialkov, Y.A., Cremona, G.H., Purtov, Y.A., Lubkowska, L., Malagon, F., Burton, Z.F., Strathern, J.N., and Kashlev, M. (2008). Transient reversal of RNA polymerase II active site closing controls fidelity of transcription elongation. Mol. Cell *30*, 557–566.

Kireeva, M., Kashlev, M., and Burton, Z.F. (2010). Translocation by multi-subunit RNA polymerases. Biochim. Biophys. Acta *1799*, 389–401.

Komissarova, N., and Kashlev, M. (1997). Transcriptional arrest: Escherichia coli RNA polymerase translocates backward, leaving the 3′ end of the RNA intact and extruded. Proc. Natl. Acad. Sci. USA *94*, 1755–1760.

Koyama, H., Ueda, T., Ito, T., and Sekimizu, K. (2010). Novel RNA polymerase II mutation suppresses transcriptional fidelity and oxidative stress sensitivity in rpb9Delta yeast. Genes Cells *15*, 151–159.

Li, S., and Smerdon, M.J. (2004). Dissecting transcription-coupled and global genomic repair in the chromatin of yeast GAL1-10 genes. J. Biol. Chem. *279*, 14418–14426.

Li, Y., Dutta, S., Doublié, S., Bdour, H.M., Taylor, J.S., and Ellenberger, T. (2004). Nucleotide insertion opposite a cis-syn thymine dimer by a replicative DNA polymerase from bacteriophage T7. Nat. Struct. Mol. Biol. *11*, 784–790.

Ljungman, M., and Zhang, F. (1996). Blockage of RNA polymerase as a possible trigger for u.v. light-induced apoptosis. Oncogene *13*, 823–831.

Marietta, C., and Brooks, P.J. (2007). Transcriptional bypass of bulky DNA lesions causes new mutant RNA transcripts in human cells. EMBO Rep. *8*, 388–393.

Mei Kwei, J.S., Kuraoka, I., Horibata, K., Ubukata, M., Kobatake, E., Iwai, S., Handa, H., and Tanaka, K. (2004). Blockage of RNA polymerase II at a cyclobutane pyrimidine dimer and 6-4 photoproduct. Biochem. Biophys. Res. Commun. *320*, 1133–1138.

Mellon, I., Spivak, G., and Hanawalt, P.C. (1987). Selective removal of transcription-blocking DNA damage from the transcribed strand of the mammalian DHFR gene. Cell *51*, 241–249.

Obeid, S., Blatter, N., Kranaster, R., Schnur, A., Diederichs, K., Welte, W., and Marx, A. (2010). Replication through an abasic DNA lesion: structural basis for adenine selectivity. EMBO J. *29*, 1738–1747.

Pomerantz, R.T., and O'Donnell, M. (2010). What happens when replication and transcription complexes collide? Cell Cycle *9*, 2537–2543.

Saxowsky, T.T., and Doetsch, P.W. (2006). RNA polymerase encounters with DNA damage: transcription-coupled repair or transcriptional mutagenesis? Chem. Rev. *106*, 474–488.

Selby, C.P., Drapkin, R., Reinberg, D., and Sancar, A. (1997). RNA polymerase II stalled at a thymine dimer: footprint and effect on excision repair. Nucleic Acids Res. *25*, 787–793.

Strauss, B.S. (1991). The 'A rule' of mutagen specificity: a consequence of DNA polymerase bypass of non-instructional lesions? Bioessays *13*, 79–84.

Taylor, J.S. (2002). New structural and mechanistic insight into the A-rule and the instructional and non-instructional behavior of DNA photoproducts and other lesions. Mutat. Res. *510*, 55–70.

van Gool, A.J., Verhage, R., Swagemakers, S.M., van de Putte, P., Brouwer, J., Troelstra, C., Bootsma, D., and Hoeijmakers, J.H. (1994). RAD26, the functional S. cerevisiae homolog of the Cockayne syndrome B gene ERCC6. EMBO J. *13*, 5361–5369.

Walmacq, C., Kireeva, M.L., Irvin, J., Nedialkov, Y., Lubkowska, L., Malagon, F., Strathern, J.N., and Kashlev, M. (2009). Rpb9 subunit controls transcription fidelity by delaying NTP sequestration in RNA polymerase II. J. Biol. Chem. *284*, 19601–19612.

Wang, D., Bushnell, D.A., Westover, K.D., Kaplan, C.D., and Kornberg, R.D. (2006). Structural basis of transcription: role of the trigger loop in substrate specificity and catalysis. Cell *127*, 941–954.

Waters, L.S., Minesinger, B.K., Wiltrout, M.E., D'Souza, S., Woodruff, R.V., and Walker, G.C. (2009). Eukaryotic translesion polymerases and their roles and regulation in DNA damage tolerance. Microbiol. Mol. Biol. Rev. *73*, 134–154.

Westover, K.D., Bushnell, D.A., and Kornberg, R.D. (2004). Structural basis of transcription: nucleotide selection by rotation in the RNA polymerase II active center. Cell *119*, 481–489.

Woudstra, E.C., Gilbert, C., Fellows, J., Jansen, L., Brouwer, J., Erdjument-Bromage, H., Tempst, P., and Svejstrup, J.Q. (2002). A Rad26-Def1 complex coordinates repair and RNA pol II proteolysis in response to DNA damage. Nature *415*, 929–933.